Competitive Formation of Inter- and Intragranularly Nucleated Ferrite

S.J. JONES and H.K.D.H. BHADESHIA

A recent trend in the development of tough steels has been to stimulate the heterogeneous nucleation of ferrite on nonmetallic particles, at the expense of that nucleated at the austenite grain surfaces. This leads to a refinement of the microstructure, which also becomes less organized, thus giving better mechanical properties. This article deals with a model for the competitive growth of ferrite nucleated both at austenite grain surfaces and intragranularly on inclusions. The classical Johnson–Mehl–Avrami theory for overall transformation kinetics has been adapted to deal with such simultaneous transformations. The theory is demonstrated to reproduce known trends in experimental observations and is shown to be of use in the design of steels.

I. INTRODUCTION

IT is well established that a refinement of the steel microstructure leads to an improvement in both the strength and toughness. Since ferrite generally nucleates at the austenite grain surfaces, the steel microstructure can be made finer by reducing the size of the austenite grains, thus providing a greater number density of nucleation sites. An alternative (or complementary) approach is to introduce additional heterogeneous nucleation sites in the form of finely dispersed and carefully chosen nonmetallic particles.[1–9] These act as sites for the intragranular nucleation of ferrite. This method has been used successfully for many decades in the welding industry,[10,11] but has recently become prominent even in wrought steels, which are inoculated with appropriate particles during the steelmaking process.[1,5–9]

A microstructure in which the ferrite is nucleated at both the austenite grain surfaces and intragranular sites also tends to be less random. It presents many more crystallographic orientations of ferrite per unit volume of sample, so that propagating cleavage cracks are frequently deflected. This leads to an improvement of toughness beyond that expected from grain refinement alone.

Much of the work in the development of steels that rely on intragranularly nucleated ferrite has been done empirically. In other contexts, attempts at modeling continuous cooling transformations involving simultaneous reactions have assumed that the different reactions occur successively.[12,13,14] The aim here was to develop an overall transformation kinetics model capable of treating the simultaneous formation of ferrite from a variety of different nucleation sites, by adapting the classic Johnson–Mehl–Avrami theory.[15]

S.J. JONES, Metallurgist, is with the Ford Motor Company, Dagenham United Kingdom, H.K.D.H. BHADESHIA, Reader in Physical Metallurgy, is with the Department of Materials Science and Metallurgy, Cambridge CB2 3QZ, United Kingdom.

Manuscript submitted July 25, 1996.

II. OVERALL TRANSFORMATION KINETICS: ISOLATED REACTIONS

A brief description of the Johnson–Mehl–Avrami theory for overall transformation kinetics is presented first, in order to highlight the enhancements suggested later; a detailed review can be found in Christian.[15]

Consider the precipitation of β from the parent phase γ. A precipitate particle can be considered to form after an incubation period τ. Assuming isotropic growth at a constant rate G, the volume v_τ of such a spherical particle is given by

$$v_\tau = (4\pi/3)G^3(t - \tau)^3 \quad (t > \tau) \qquad [1]$$

$$v_\tau = 0 \quad (t < \tau) \qquad [2]$$

where t is the time defined to be zero at the instant the sample reaches the isothermal transformation temperature.

Particles nucleated at different locations may eventually touch. This problem of hard impingement is neglected at first, by allowing particles to grow through each other and by permitting nucleation to happen even in regions that have already transformed. The calculated volume of β phase is therefore an *extended volume*; the change in extended volume due to particles nucleated in a time interval τ to $\tau + d\tau$ is, therefore, given by

$$dV_\beta^e = v_\tau I V d\tau$$

i.e.

$$V_\beta^e = (4\pi V/3)\int_{\tau=0}^{t} G^3 I(t - \tau)^3 d\tau \qquad [3]$$

where I is the nucleation rate per unit volume and $V = V_\gamma + V_\beta$ is the total sample volume. The term V_γ is the volume of untransformed γ at any instant.

Only those parts of the change in extended volume that lie in untransformed regions of the parent phase can contribute to the change in the real volume of β. If nucleation occurs randomly in the parent material, then the probability that any change in the extended volume lies in untransformed parent phase is proportional to the fraction of untransformed material at that instant. It follows that the real change in volume in the time interval t to $t + dt$ is

$$dV_\beta = (1 - \frac{V_\beta}{V}) dV^e_\beta$$

$$V^e_\beta = -V \ln (1 - \frac{V_\beta}{V})$$

so that

$$- \ln (1 - \frac{V_\beta}{V}) = (4\pi/3) G^3 \int_0^t I(t - \tau)^3 d\tau$$

In making this conversion from extended to real volume, all information about individual particles is lost, so that the application of the Avrami model yields only the volume fraction transformed. Equation [3] can be integrated with specific assumptions about the nucleation rate, when the nucleation rate is constant:

$$\zeta_\beta = \frac{V^\beta}{V} = 1 - \exp(-\pi G^3 I t^4/3) \qquad [4]$$

where ζ_β is the volume fraction of β. This is the form of the classic Johnson–Mehl–Avrami equation that can be adapted for a variety of nucleation and growth phenomena. The theory is, however, restricted to the precipitation of a single phase from the parent. We now proceed to illustrate how it can be modified to treat the occurrence of two or more simultaneous reactions.

III. SIMULTANEOUS REACTIONS WITH RANDOM NUCLEATION

A. *Analytical Illustration*

Consider first a case in which α and β precipitate at the same time from the parent phase, which is designated γ. It is assumed that the nucleation and growth rates do not change with time and that the particles grow isotropically. The increase in the extended volume due to particles nucleated in a time interval $t = \tau$ to $t = \tau + d\tau$ is, therefore, given by

$$dV^e_\alpha = \frac{4}{3} \pi G^3_\alpha (t - \tau)^3 I_\alpha V \, d\tau \quad \text{and}$$
$$dV^e_\beta = \frac{4}{3} \pi G^3_\beta (t - \tau)^3 I_\beta V \, d\tau \qquad [5]$$

where G_α, G_β, I_α, and I_β are the growth and nucleation rates of α and β, respectively, all of which are assumed here to be independent of time. $V = V_\gamma + V_\alpha + V_\beta$ is the total volume of the system. For each phase, the increase in extended volume will consist of three separate parts. Thus, for α, the parts are

(1) α that forms in untransformed γ,
(2) α that forms in existing α, and
(3) α that forms in existing β.

Only α formed in untransformed γ will contribute to the real volume of α. On average, a fraction $[1 - (V_\alpha + V_\beta)/V)]$ of the extended volume will be in previously untransformed material. It follows that the increase in real volume of α in the time interval t to $t + dt$ is given by

$$dV_\alpha = \left(1 - \frac{V_\alpha + V_\beta}{V}\right) dV^e_\alpha \text{ and similarly for } \beta,$$

$$dV_\beta = \left(1 - \frac{V_\alpha + V_\beta}{V}\right) dV^e_\beta$$

In general, V_α will be some complex function of V_β, and it is not possible to integrate these expressions to find the relationship between the real and extended volumes. However, in certain simple cases, it is possible to relate V_α to V_β by multiplication with a suitable constant, K, in which case $V_\beta = KV_\alpha$. The equations relating the increment in the real volume to that of the extended volume can therefore be written as

$$dV_\alpha = \left(1 - \frac{V_\alpha + KV_\alpha}{V}\right) dV^e_\alpha \quad \text{and}$$
$$dV_\beta = \left(1 - \frac{V_\beta + KV_\beta}{KV}\right) dV^e_\beta \qquad [6]$$

They may then be integrated to find an analytical solution relating the extended and real volumes analogous to that for single-phase precipitation.

$$\frac{V^e_\alpha}{V} = \frac{-1}{1 + K} \ln \left[1 - \frac{V_\alpha}{V}(1 + K)\right] \quad \text{and}$$
$$\frac{V^e_\beta}{V} = \frac{-K}{1 + K} \ln \left[1 - \frac{V_\beta}{V}\left(\frac{1 + K}{K}\right)\right] \qquad [7]$$

The total extended volume fraction is found for each phase by integrating Eq. [5] with respect to τ. This gives

$$\zeta_\alpha = \left(\frac{1}{1 + K}\right)\left(1 - \exp\left[-\frac{1}{3}(1 + K)\, \pi G^3_\alpha I_\alpha t^4\right]\right) \qquad [8]$$

$$\zeta_\beta = \left(\frac{K}{1 + K}\right)\left(1 - \exp\left[-\frac{1}{3}\left(\frac{1 + K}{K}\right) \pi G^3_\beta I_\beta t^4\right]\right) \qquad [9]$$

These equations resemble the well-known Avrami equation for single-phase precipitation, with additional factors to account for the second precipitate phase. When the fractions of both precipitating phases are small, the equations approximate to the expressions for each phase precipitating alone. This is because nearly all of the extended volume then lies in previously untransformed material and contributes to the real volume. It is possible for constant nucleation and growth rates to calculate explicitly the value of K, which is given by

$$K = V_\beta/V_\alpha = (I_\beta G^3_\beta)/(I_\alpha G^3_\alpha)$$

Some example calculations for the case of constant growth rate are presented in Figure 1. When the nucleation and growth rates of α and β are set to be identical, their transformation curves superimpose and each phase eventually achieves a maximum fraction of 0.5 (Figure 1(a)). When the nucleation rate of β is set to be twice that of α, then for identical growth rates, the terminal fraction of β is twice that of α (Figure 1(b)). The case where the growth rate of β is set to be twice that of α (with identical nucleation rates) is illustrated in Figure 1(c). The final volume fraction of the β phase is then 8 times that of the α phase, because volume fraction is a function of the growth rate

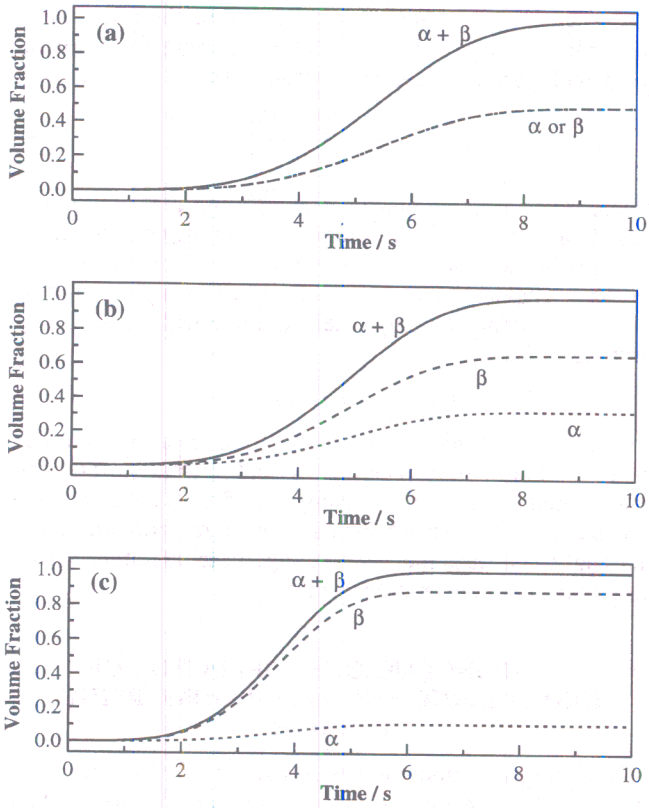

Fig. 1—An illustration of the kinetics of two reactions occurring simultaneously, both of which nucleate randomly and grow in a linear manner: (*a*) when the two phases have identical nucleation and growth rates. (*b*) identical growth rates but with the β having twice the nucleation rate of α; and (*c*) identical nucleation rates but with β particles growing at twice the rate of the α particles.

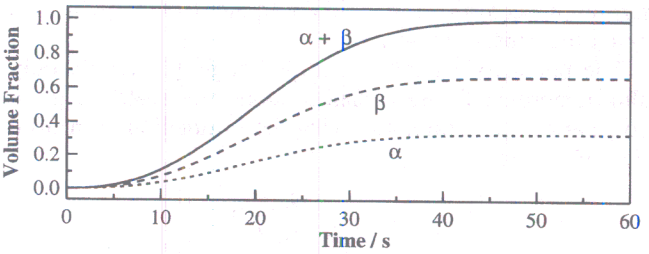

Fig. 2—An illustration of the kinetics of two reactions occurring simultaneously, both of which nucleate randomly and grow in a parabolic manner. Phase β has twice the nucleation rate of α (both phases have similar growth characteristics).

cubed. Note that the analytical method shown previously can be extended to allow for any number of simultaneously precipitating phases.

The growth rate need not be constant. In diffusion-controlled growth, the particle dimension will vary with the square root of time, the constant of proportionality being the three-dimensional parabolic thickening rate constant (ξ). The value of ξ remains constant as long as the far-field concentration in the matrix does not change. Therefore, Eqs. [1] and [2] are rewritten as

$$v_\tau = (4\pi/3)\xi^3(t - \tau)^{3/2} \quad (t > \tau) \qquad [10]$$

$$v_\tau = 0 \qquad (t < \tau) \qquad [11]$$

so that Eq. [5] becomes

$$dV^e_\alpha = \frac{4}{3}\pi\xi^3_\alpha (t - \tau)^{3/2} I_\alpha V\, d\tau \quad \text{and}$$
$$dV^e_\beta = \frac{4}{3}\pi\xi^3_\beta (t - \tau)^{3/2} I_\beta V\, d\tau \qquad [12]$$

where ξ_α and ξ_β are the three-dimensional parabolic thickening rate constants of α and β, respectively. Therefore, the volume fractions of α and β at time t are given by

$$\zeta_\alpha = \left(\frac{1}{1 + K}\right)\left(1 - \exp\left[-\frac{.8}{15}(1 + K)\,\pi\xi^3_\alpha I_\alpha t^{5/2}\right]\right) \qquad [13]$$

$$\zeta_\beta = \left(\frac{K}{1 + K}\right)\left(1 - \exp\left[-\frac{8}{15}\left(\frac{1 + K}{K}\right)\pi\xi^3_\beta I_\beta t^{5/2}\right]\right) \qquad [14]$$

where the value of K is obtained from

$$K = V_\beta/V_\alpha = (I_\beta\xi^3_\beta)/(I_\alpha\xi^3_\alpha)$$

Figure 2 illustrates the case when β nucleates at twice the rate of α and $\xi_\alpha = \xi_\beta$. It is emphasized that these analytical relations are valid only if the values of ξ do not change during transformation, *i.e.*, at very small degrees of transformation.

B. *Numerical Solution*

While the analytical method is more transparent, a numerical procedure is more versatile when the boundary conditions for nucleation and growth change during transformation. Consider a system with n precipitating phases, which nucleate randomly and grow *via* their individual mechanisms. The change in the real volume of phase j in the current time interval t to $t + \Delta t$ is

$$\Delta V_j = \left(1 - \frac{\Sigma^n_{i=1} V_i}{V}\right)\Delta V^e_j \qquad [15]$$

where ΔV^e_j is the corresponding change in the extended volume of phase j in the same time interval, V_i is the real volume of the ith phase at time t, and V is the total volume of the assembly, ΔV^e_j may have a contribution from particles nucleated during the period $t = 0$ to $t = m\Delta t$, where m is an integer such that $m\Delta t$ is the current time t, so that

$$\Delta V^e_j = \sum_{k=0}^{m} (V I_{j,k}\Delta\tau)(v_{j,k}\Delta t)$$

where $v_{j,k}$ is the rate of change of extended volume of a particle of phase j, which nucleated between $k\Delta\tau$ and $(k + 1)\Delta\tau$, during the current time interval $m\Delta t$ to $(m + 1)\Delta t$. $I_{j,k}$ is the nucleation rate per unit volume of phase j during the time interval $k\Delta\tau$ to $(k + 1)\Delta\tau$. $VI_{j,k}\Delta\tau$ is the number of extended particles of j nucleated in this time interval. The terms Δt and $\Delta\tau$ are taken to be numerically identical.

The instantaneous value of ΔV_j, together with the corresponding changes in the real volumes of the other $n - 1$ phases, is used to update the total real volume of each phase at time $t + \Delta t$ in a computer implemented numerical procedure by writing

$$V_{j,t+\Delta t} = V_{j,t} + \Delta V_j \quad \text{for} \quad j = 1 \ldots n$$

so that a plot of the real volume of each phase can be obtained as a function of time. The growth and nucleation

rates can also be updated during this step, should they have changed because of solute enrichment in the untransformed parent material or because there is a change in temperature during continuous cooling transformation.

IV. SIMULTANEOUS REACTIONS—BOUNDARY NUCLEATED

The analysis presented subsequently is a numerical adaptation for simultaneous reactions of the general method of Cahn and Avrami,[15] in which there are two applications of extended space, the first applying to the gradual elimination of free grain boundary area and the second to the gradual elimination of volume of untransformed material.[15] If we consider a planar boundary of area O_B (which is equal to the total grain boundary area per unit volume in the assembly) in a system with n precipitating phases, where $O_{i,y}$ is the total real area intersected by the ith phase on a plane parallel to the boundary but at a distance y normal to that boundary at time t, we have for the jth phase,

$$\Delta O_{j,y} = \left(1 - \frac{\Sigma_{i=1}^{n} O_{i,y}}{O_B}\right) \Delta O^e_{j,y} \qquad [16]$$

where $\Delta O_{j,y}$ is the change in the real area intersected with the plane at y by phase j, during the small time interval t to $t + \Delta t$. $\Delta O^e_{j,y}$ is similarly the change in the extended area of intersection with the same plane at y. This may have a contribution from particles nucleated throughout the period $t = 0$ to $t = m\Delta t$, where m is an integer such that $m\Delta t$ is the current time t, so that

$$\Delta O^e_{j,y} = \sum_{k=0}^{m} (O_B I_{j,k} \Delta\tau)\ (A_{j,k,y} \Delta t)$$

where $A_{j,k,y}$ is the rate of change of the extended area of intersection on plane y of a particle of phase j, which nucleated between $k\Delta\tau$ and $(k + 1)\Delta\tau$, during the current time interval $m\Delta t$ to $(m + 1)\Delta t$. The term $I_{j,k}$ is the nucleation rate per unit area of phase j during the time interval $k\Delta\tau$ to $(k + 1)\Delta\tau$. $O_B I_{j,k} \Delta\tau$ is the number of extended particles nucleated in this time interval. Note that Δt and $\Delta\tau$ are taken to be numerically identical. Then, $\Delta O_{j,y}$ is used to update the total real area of intersection of phase j with the same plane at y at time $t + \Delta t$ by writing

$$O_{j,y,t+\Delta t} = O_{j,y,t} + \Delta O_{j,y} \quad \text{for} \quad j = 1 \ldots n$$

To obtain a change in the extended volume of phase j on one side of the boundary, it is necessary to integrate as follows:

$$dV^e_j = \int_{y=0}^{q_j^{\max}} dO_{j,y} dy$$

where $dO_{j,y}$ is equivalent to $\Delta O_{j,y}$ and $q_j^{\max}$ is the maximum extended size of a particle of phase j in a direction normal to the grain boundary plane. Thus, the change in the extended volume of phase j on one side of the boundary in the time interval t to $t + \Delta t$ may be numerically evaluated as

$$\Delta V^e_j = \Delta y \sum_{y=0}^{q_j^{\max}} \Delta O_{j,y} \qquad [17]$$

where Δy is a small interval in y. Therefore, the corresponding change in the real volume after allowing for impingement with particles originating from other boundaries is

$$\Delta V_j = \left(1 - \frac{\Sigma_{i=1}^{n} V_i}{V}\right) \Delta V^e_j \qquad [18]$$

where V_i is the real volume of the ith phase at time t. The instantaneous value of ΔV_j, together with the corresponding changes in the volumes of the other $n - 1$ phases, can be used to calculate the total real volume of each phase at time $t + \Delta t$ in a computer implemented numerical procedure by writing

$$V_{j,t+\Delta t} = V_{j,t} + \Delta V_j \quad \text{for} \quad j = 1 \ldots n$$

so that a plot of the fraction of each phase can be obtained as a function of time. The growth and nucleation rates can also be updated during this step, should they have changed because of solute enrichment in the untransformed parent material or because there is a change in temperature during continuous cooling transformation.

V. SIMULTANEOUS FORMATION OF IDIOMORPHIC AND ALLOTRIOMORPHIC FERRITE

Modeling the simultaneous formation of both intra- and intergranularly nucleated allotriomorphic ferrite is then straightforward using equations very similar to those discussed earlier. In this case, only one phase is forming, however, it is nucleating at two very different types of site. So that henceforth the subscript $j = 1$ is used to distinguish allotriomorphic ferrite nucleated at the austenite grain boundaries from intragranularly nucleated allotriomorphic ferrite (henceforth termed idiomorphic ferrite), which is given the subscript $j = 2$.

The boundary model is modified slightly, because only allotriomorphic ferrite nucleates along the austenite grain boundaries. Therefore, removing the summation term from Eq. [16] gives

$$\Delta O_{1,y} = \left(1 - \frac{O_{1,y}}{O_B}\right) \Delta O^e_{1,y}$$

The competition between allotriomorphic and idiomorphic ferrite particles for the untransformed austenite is modeled by using Eq. [18] (where j has been redefined as shown previously) to calculate how the real volumes of allotriomorphic and idiomorphic ferrite change during each time interval.

The nucleation and growth of allotriomorphic ferrite has been described by modeling the allotriomorphs as discs having their faces parallel to the nucleating grain boundary plane.[12,13] The discs are assumed to grow on both sides of the parent boundary under paraequilibrium conditions, so that the half-thickness q_1 of each disc during isothermal growth is given by

$$q_1 = \zeta(t - \tau)^{1/2} \qquad [19]$$

where ζ is the one-dimensional parabolic thickening rate constant. The growth rate slows down as the concentration gradient ahead of the moving interface decreases to accommodate the carbon that is partitioned into the austenite. The

growth rate parallel to the grain boundary plane is taken to be 3 times that normal to it, giving a constant aspect ratio η_1 of 3.0, so that the disc radius is $\eta_1 q_1$.[16] For nonisothermal growth, the change in thickness during a time interval dt is given by differentiating Eq. [19] to give

$$dq_1 = \frac{1}{2}\zeta(t - \tau)^{-1/2}\, dt$$

Therefore, for a particle nucleated between $k\Delta\tau$ and $(k + 1)\Delta\tau$, the half-thickness at the current time $(m + 1)\Delta t$ is evaluated numerically as

$$q_{1,(m+1)\Delta t} = q_{1,m\Delta t} + \frac{1}{2}\zeta(m\Delta t - k\Delta\tau)^{-1/2}\,\Delta t$$

The rate of change of area of intersection on a plane y of a disc of allotriomorphic ferrite nucleated between $k\Delta\tau$ and $(k + 1)\Delta\tau$, during the current time interval $m\Delta t$ to $(m + 1)\Delta t$, is taken as

$$\begin{aligned} A_{1,k,y} &= \pi\eta_1^2\zeta^2 && (q_{1,(m+1)\Delta t} > y) \\ A_{1,k,y} &= \pi\eta_1^2 q_{1,(m+1)\Delta t}^2/\Delta t && (q_{1,(m+1)\Delta t} = y) \\ A_{1,k,y} &= 0 && (q_{1,(m+1)\Delta t} < y) \end{aligned}$$

Since the ferrite allotriomorphs can grow into both of the adjacent austenite grains, if follows from Eq. [17] that

$$\Delta V_1^e = 2\Delta y \sum_{y=0}^{q_1^{\max}} \Delta O_{1,y} \qquad [20]$$

The random nucleation and growth of idiomorphic ferrite on nonmetallic particles has been described by modeling the allotriomorphs as spheres, which grow parabolically under paraequilibrium conditions. For nonisothermal growth, the rate of change of extended volume of a particle of idiomorphic ferrite, which nucleated at $\tau = k\Delta\tau$ during the time current interval $t = m\Delta t$ to $t = (m + 1)\Delta t$, is

$$\begin{aligned} \upsilon_{2,k} &= 2\pi\xi^3(m\Delta t - k\Delta\tau)^{1/2} && (m\Delta t > k\Delta\tau) \\ \upsilon_{2,k} &= \frac{4}{3}\pi\xi^3\Delta t^{1/2} && (m\Delta t = k\Delta\tau) \end{aligned}$$

where ξ is the three-dimensional parabolic thickening constant.

Classical nucleation theory is used to model the nucleation rate of allotriomorphic ferrite on the austenite grain boundaries, with the nucleation rate per unit area of boundary given by an equation of the form

$$I_1 = C_a \frac{kT}{h} \exp\{-\frac{G_1^* + Q}{RT}\} \exp\{-\frac{\tau^*}{t}\} \qquad [21]$$

where h is the Planck constant, k is the Boltzmann constant, T is the absolute temperature, and R is the universal gas constant. The term Q is a constant activation energy representing the barrier to the transfer of atoms across the interface; it should have a value smaller than that for the self-diffusion of iron in austenite (270 kJ mol^{-1}[17]), since it involves the diffusion of atoms across a defect (boundary) as opposed to diffusion in the defect-free lattice. The activation energy for nucleation is given by $G_1^* = C_b\sigma^3/\Delta G^2$, where σ is an effective interfacial energy per unit area, discussed subsequently. The term ΔG is the maximum chemical free energy change per unit volume available for nucleation.[18] The second exponential term relates to the achievement of a steady-state nucleation rate: $\tau^* = n_c^2 h(4a_c kT)^{-1} \exp\{Q/RT\}$, where n_c is the number of atoms in the critical nucleus and a_c is the number of atoms in the critical nucleus, which are at the interface;[15] these quantities are a function of σ and ΔG and were calculated assuming a spherical shape.

The equation contains three unknowns about the nucleation of allotriomorphic ferrite, all of which have to be determined experimentally. Annelli *et al.*[14] have published some careful experimental data on the evolution of the fraction of allotriomorphic ferrite as a function of the austenite grain size, chemical composition, and transformation temperature. Equation [21] was fitted to these data to obtain the unknown quantities. We now return to the term designated the effective surface energy σ. A real nucleus will be bounded by a number of interfaces, each of different interfacial energy, and the shape will depend also on that of the austenite grain boundary on which heterogeneous nucleation occurs. None of these details are known, but it is relevant to note that the form of Eq. [21] is preserved even for heterogeneous nucleation. Furthermore, the assumed value of σ (0.025 J m^{-2}) is not overly significant since it is multiplied by the empirical fitting constant C_a. This constant C_a may be regarded as a correction to the real interfacial energy, but it also represents the shape of the nucleus, which is not defined. For the purposes of the present work, the values $C_a = 4.86 \times 10^{10}$ m^{-2}, $C_b = 4.19$, and $Q = 200$ kJ mol^{-1} were found to give a good fit to the experimental data of Reference 14. We note that as expected, Q is smaller than the activation energy for self-diffusion in austenite.

It is emphasized here that there is considerable complexity in the detail of nucleation theory, which has been neglected here because the parameters necessary cannot be derived with confidence from existing experimental data. For example, the interfacial energy is unlikely to be isotropic, it may vary with size, and there will be a dependence of the shape on the defect on which nucleation occurs.[15] The austenite grain surfaces themselves cannot be assumed to have a constant interfacial energy. The parameters stated here in order to model nucleation are therefore of limited value. This issue arises in all kinetic theory and is not a problem unique to the model presented here. The value of Q is, however, reasonable. The purpose of this work is to demonstrate that the simultaneous transformations can be properly represented in overall transformation kinetics, rather than to deduce nucleation functions.

The nucleation rate of idiomorphic ferrite on nonmetallic particles per unit volume is similarly obtained, this time by fitting the following equation to the data by Ueda *et al.*:[19]

$$I_2 = C_c N_V \frac{kT}{h} \exp\{-\frac{G_2^* + Q}{RT}\} \exp\{-\frac{\tau^*}{t}\} \qquad [22]$$

where $C_c = 0.0955$ is a fitted constant and N_V is the number of nonmetallic particles per unit volume. $G_2^* = C_d\sigma^3/\Delta G^2$, where $C_d = 7.54$, is a fitted constant (this value is consistent with the generally accepted view that inert inclusions are less potent sites for nucleation than the austenite grain boundaries).

The one-dimensional parabolic thickening constant is obtained by solving[15]

Table I. The Chemical Compositions (Weight Percent) of the Steels Studied by Ueda *et al.*[19]

Alloy	C	Si	Mn	B	N	Comment
b	0.12	0.25	1.47	—	0.0045	boron-free steel
c	0.12	0.23	1.44	0.0029	0.0074	high nitrogen, boron steel
d	0.13	0.23	1.45	0.0030	0.0014	low nitrogen, boron steel

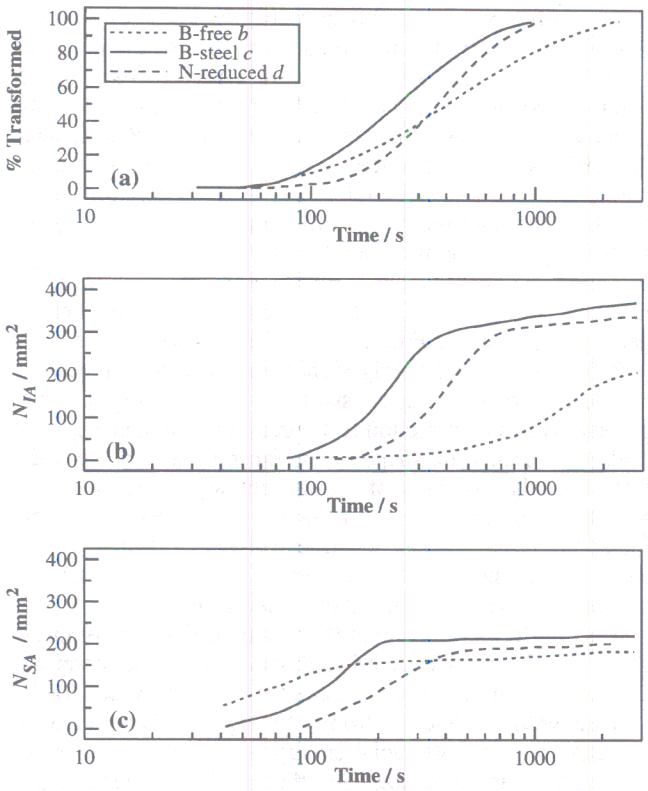

Fig. 3—Experimental data reported by Ueda *et al.* for the alloys listed in Table I:[19] (*a*) total normalized fraction of transformation as a function of time at 720 °C, following austenitization at 1350 °C for 10 s; (*b*) number density N_{IA} of ferrite grains observed to grow from intragranular nucleation sites; and (*c*) number density N_{SA} of ferrite grains observed to grow from austenite grain surfaces.

$$2\left(\frac{\underline{D}}{\pi}\right)^{1/2}\Omega = \zeta \exp\left\{\frac{\zeta^2}{4\underline{D}}\right\} \operatorname{erfc}\left\{\frac{\zeta}{2\underline{D}^{1/2}}\right\}$$

$$\text{with } \Omega = \frac{x^{\gamma\alpha} - \bar{x}}{x^{\gamma\alpha} - x^{\alpha\gamma}}$$

where $x^{\gamma\alpha}$ and $x^{\alpha\gamma}$ are the paraequilibrium carbon concentrations in austenite and ferrite, respectively, at the interface (obtained using a calculated multicomponent phase diagram), $\bar{x}$ is the average carbon concentration of the austenite, and $\underline{D}$ is a weighted average diffusivity[20,21] of carbon in austenite, given by

$$\underline{D} = \int_{x^{\gamma\alpha}}^{\bar{x}} \frac{D\{x\}\, dx}{\bar{x} - x^{\gamma\alpha}}$$

where D is the diffusivity of carbon in austenite at a particular concentration of carbon. The three-dimensional parabolic thickening constant is given by[15]

Table II. Parameters Necessary to Compare Experimental Data[19] against Theory, Together with Those Used to Predict the TTT Curves for Allotriomorphic Ferrite in Two Model Steels*

Steel	d_γ/μm	C_b	V_I	d_I/μm	C_d
b	195	4.19	2.3×10^{-5}	0.02	7.54
c	195	4.86	2.3×10^{-4}	0.02	7.54
d	177	5.53	7.8×10^{-5}	0.02	7.54
Model steel *e*	45	4.19	0	—	—
Model steel *f*	45	4.19	2.0×10^{-3}	0.5	7.54

*The term d_γ is the austenite grain size (mean lineal intercept), V_I the volume fraction of nucleating particles, and d_I the particle diameter.

$$\xi = \left[\frac{2\underline{D}\,(\bar{x} - x^{\gamma\alpha})}{x^{\alpha\gamma} - \bar{x}}\right]^{1/2}$$

VI. RESULTS AND DISCUSSION

The model described previously was validated in two ways: first, by a comparison against published experimental data; and second, by examining the predicted trends to ensure consistency with metallurgical expectations.

There is one quantitative study on the balance between idiomorphic and allotriomorphic ferrite, due to Ueda *et al.*[19] and Funakoshi *et al.*,[22] who studied transformation in the three steels listed in Table I. Using their designations, steel *b* is a mild steel, which is free of boron; and steels *c* and *d* both contain deliberate additions of boron, but the latter has an exceptionally low nitrogen concentration. Transformation in all of the alloys occurs to varying degrees, by heterogeneous nucleation at the austenite grain surfaces or intragranularly at nonmetallic particles. Ueda *et al.* thought that these particles were boron nitrides. Iron borocarbides were also suspected of inducing a small number of nucleation events. The key features of this series of steels are illustrated in Figure 3 and can be summarized as follows.

(1) The boron-free steel *b* can be regarded as the reference material with transformation originating mostly from the austenite grain surfaces.
(2) Transformation in the boron-containing high-nitrogen steel *c* is dominated by intragranular nucleation at boron nitride particles. A relatively small amount of soluble boron segregates to the austenite grain surfaces, making them slightly less effective as heterogeneous nucleation sites.
(3) The boron-containing low-nitrogen steel *d* contains a high concentration of soluble boron, which segregates to the austenite grain surfaces, making them significantly less effective as heterogeneous nucleation sites. A small increase in the number density of intragranular nucleation sites occurs because some boron nitride precipitation is inevitable.

The model requires values for certain parameters, which are steel dependent. These are listed in Table II. The austenite grain sizes are from Funakoshi *et al.*;[22] they influence the number density of grain boundary nucleation sites. The term C_b occurs in the activation energy for nucleation, with $G_1^* = C_b\sigma^3/\Delta G^2$. As stated earlier, the value of the austenite-ferrite interfacial energy per unit area (σ) was

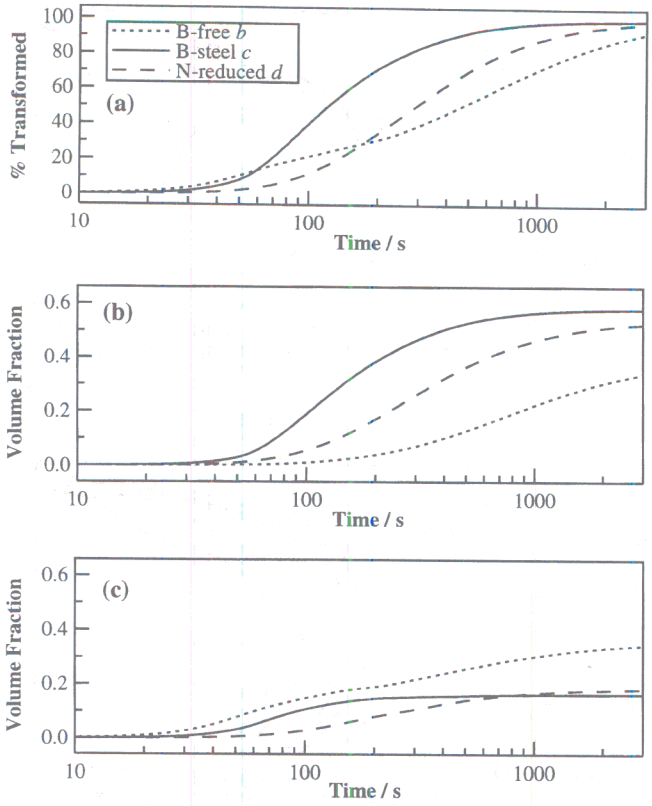

Fig. 4——Calculated data for the steels listed in Table I: (*a*) total normalized fraction of transformation as a function of time at 720 °C; the normalization is performed by dividing the calculated volume fraction transformed by the calculated paraequilibrium volume fraction of ferrite at 720 °C. (*b*) Absolute volume fraction of intragranularly nucleated idiomorphic ferrite. (*c*) Absolute volume fraction of grain boundary nucleated allotriomorphic ferrite.

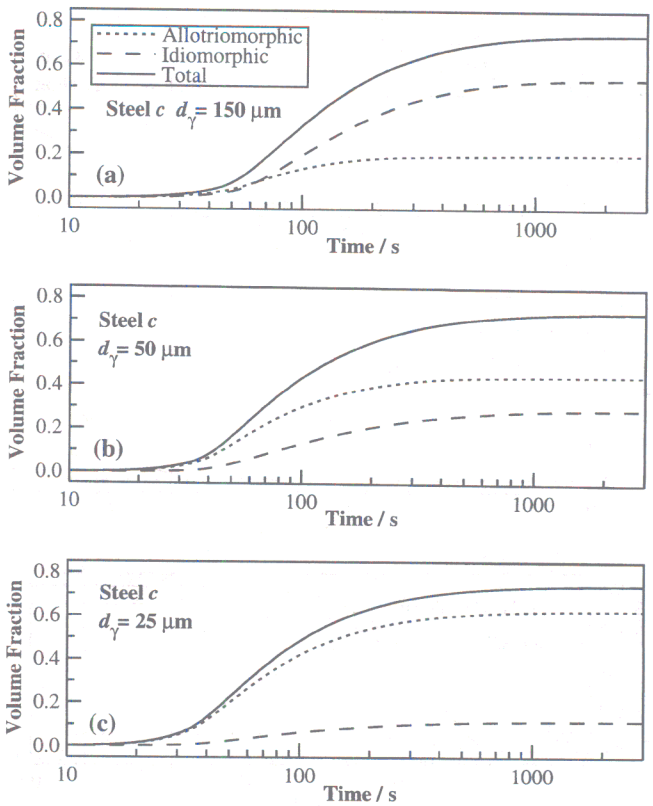

Fig. 5—Transformations in steel *c*: (*a*) an austenite grain size of 150 μm; (*b*) an austenite grain size of 50 μm; and (*c*) an austenite grain size of 25 μm.

taken to be 0.025 J m^{-2}. However, boron modifies this energy; the modification is taken into account using the data by Ueda *et al.*,[19] by adjusting empirically the value of C_b in a way consistent with the increasing quantities of soluble boron in steels *b*, *c*, and *d*. Thus, complete saturation of the boundary with boron corresponds to a value of C_b = 5.53 (Table II). In the boron-containing steels *c* and *d*, the volume fraction of nucleating particles V_I was estimated as the equilibrium volume fraction of boron nitride. This was calculated using the solubility product of boron nitride in austenite due to Maitrepierre *et al.*,[23] for the transformation temperature 720 °C. The boron nitride particle size is unknown but was taken as 0.02 μm.[24] In the boron-free steel *b*, the volume fraction of nucleating particles was assumed to be an order of magnitude less than the calculated volume fraction of boron nitride in steel *c*. The particle size was assumed to be the same as that in steels *c* and *d*.

Figure 4 shows the transformation curves estimated for steels *b*, *c*, and *d*; these can be compared against the experimental curves given in Figure 3. It should, however, be borne in mind that Figures 3(b) and (c) are plots of the number densities of intragranular or boundary particles, rather than the volume fractions plotted in Figure 4.

Isothermal transformation at 720 °C can only continue until the equilibrium volume fraction is reached, leaving some austenite untransformed. To allow a comparison against the experimental data, which are in effect normalized with respect to the equilibrium fraction, Figure 4(a) has been similarly normalized. It is clear that all the trends evident in the experimental transformation curves are reproduced faithfully. Examination of Figures 4(b) and (c) shows that consistent with the experimental data (Figures 3(b) and (c)) grain boundary transformation dominates in the boron-free steel *b*. The reverse is true for the boron-rich high-nitrogen steel *c*, where the boron nitride particles stimulate intragranular transformation and soluble boron retards grain boundary allotriomorph nucleation. As expected, the suppression of allotriomorphic ferrite is largest for the low-nitrogen boron steel *d*.

These results are encouraging given that the only parameter that has been adjusted to distinguish the steels is the value of C_b, which alters the potency of the austenite grain boundaries to account for the differing levels of soluble boron. The model was further tested to ensure that it was consistent with metallurgical expectations.

A reduction in the austenite grain size should lead to a change in the balance between allotriomorphic and idiomorphic ferrite. This is illustrated in Figure 5 for steel *c*, where data are presented for austenite grain sizes of 150, 50, and 25 μm. The reduction in the austenite grain size leads to a change from an idiomorphic to allotriomorphic ferrite dominated transformation. Such an effect is well established from a qualitative point of view;[10] large austenite grain sizes favor intragranularly nucleated transformation products for two reasons. First, the number density of grain boundary nucleation sites decreases relative to intragranular sites as d_γ is increased. Second, grain boundary nucleation sites are generally more potent than inclusions, so transformation commences first at the boundaries. Therefore, assuming a constant thickness of allotriomorphic ferrite along

phic ferrite continues over the full course of the transformation because the nonmetallic inclusions are randomly distributed throughout the volume of the assembly. Therefore, all of the extended particles of idiomorphic ferrite that are nucleated during the course of the transformation can contribute to the real volume. Furthermore, these intragranularly nucleated ferrite particles grow more rapidly due to the three-dimensional diffusion of carbon in the austenite around them. Consequently, while the overall transformation rate is increased in a manner consistent with the greater density of nucleation sites, the later stages of transformation are greatly accelerated by contributions from intragranularly nucleated idiomorphic ferrite.

VII. SUMMARY

An overall transformation kinetics model has been produced for dealing with the simultaneous formation of allotriomorphic and idiomorphic ferrite. It has been possible to reproduce experimentally observed trends in published data, and the analysis gives insight into the competing effects of inter- and intragranular nucleation sites. These methods can be used in the design of new steels. Furthermore, this approach can easily be extended to allow for the simultaneous inter- and intragranular nucleation of a variety of phases, such as allotriomorphic ferrite, Widmanstätten ferrite, bainite, and pearlite.[25] Therefore, it should be possible to model the transformation kinetics of quite complex systems such as low-alloy steel weld metals.

ACKNOWLEDGMENTS

We are grateful to the Engineering and Physical Sciences Research Council and British Steel plc. for supporting this work. It is a pleasure to acknowledge some very helpful discussions with Dr Graham Thewlis. HKDHB is grateful to the Royal Society for a Leverhulme Trust Senior Research Fellowship.

REFERENCES

1. M. Imagumbai, R. Chijiiwa, N. Aikawa, M. Nagumo, H. Homma, S. Matsuda, and H. Mimura: in *HSLA Steels: Metallurgy and Applications*, J.M. Gray, T. Ko, Z. Shouhua, W. Baorong, and X. Xishan, eds., ASM INTERNATIONAL, Metals Park, OH, 1985, pp. 557-66.
2. Y. Ito and M. Nakanishi: *Sumitomo Search*, 1976, vol. 15, pp. 42-62.
3. D.J. Abson and R.J. Pargeter: *Int. Met. Rev.*, 1986, vol. 31, pp. 141-94.
4. H.K.D.H. Bhadeshia: *Bainite in Steels*, Institute of Materials, London, 1992, pp. 245-90.
5. T. Ochi, T. Takahashi, and H. Takada: *30th Mechanical Working and Steel Processing Conf.*, Iron and Steel Society, Warrendale, PA, 1988, pp. 1-12.
6. F. Ishikawa, T. Takahashi, and T. Ochi: *Metall. Mater. Trans. A*, 1994, vol. 25A, pp. 929-36.
7. F. Ishikawa and T. Takahashi: *Iron Steel Inst. Jpn. Int.*, 1995, vol. 35, pp. 1128-33.
8. M.A. Linaza, J.L. Romero, J.M. Rodriguez-Ibabe, and J.J. Urcola: *Scripta Metall. Mater.*, 1993, vol. 29, pp. 1217-22.
9. M.A. Linaza, J.L. Romero, J.M. Rodriguez-Ibabe, and J.J. Urcola: *Scripta Metall. Mater.*, 1995, vol. 32, pp. 395-400.
10. H.K.D.H. Bhadeshia and L.-E. Svensson: in *Mathematical Modelling in Weld Phenomena*, H. Cerjak and K.E. Easterling, ed., Institute of Materials, London, 1993, pp. 109-82.
11. *ϕ*. Grong: *Metallurgical Modelling of Welding*, Institute of Materials, London, 1994, pp. 387-475.
12. M. Umemoto, A. Hiramatsu, A. Moriya, T. Watanabe, S. Nanba, N. Nakahima, G. Anan, and Y. Higo: *Iron Steel Inst. Jpn. Int.*, 1992, vol. 32, pp. 302-15.
13. H.K.D.H. Bhadeshia, L.-E. Svensson, and B. Gretoft: *Acta Metall.*, 1985, vol. 33, pp. 1271-83.
14. E. Anelli, S. Amato, and P.E. Di-Nunzio: *European Steel and Coal Community Report 7769R*, Centro Sviluppo Materiali, Rome, 1991.
15. J.W. Christian: *Theory of Transformations in Metals and Alloys*, 2nd ed., Part I, Pergamon Press, Oxford, United Kingdom, 1975.
16. J.R. Bradley and H.I. Aaronson: *Metall. Trans. A*, 1977, vol. 8A, pp. 317-22.
17. F.S. Buffington, K. Hirano, and M. Cohen: *Acta Metall.*, 1961, vol. 9, pp. 434-39.
18. H.K.D.H. Bhadeshia: *Met. Sci.*, 1982, pp. 159-65.
19. S. Ueda, M. Ishikawa, and N. Ohashi: in *Boron in Steels*, S.K. Banerji and J.E. Morral, eds., TMS-AIME, Warrendale, PA, 1980, pp. 181-98.
20. R. Trivedi and G.R. Pound: *J. Appl. Phys.*, 1967, vol. 38, pp. 3569-76.
21. H.K.D.H. Bhadeshia: *Met. Sci.*, 1981, vol. 15, pp. 477-79.
22. T. Funakoshi, T. Tanaka, S. Ueda, M. Ishikawa, N. Koshizuka, and N. Kobayashi: *Trans. Iron Steel Inst. Jpn.*, 1976, pp. 419-27.
23. P. Maitrepierre, J. Rofes-Vernis, and D. Thivellier: in *Boron in Steels*, S.K. Banerji and J.E. Morral, eds., TMS-AIME, Warrendale, PA, 1980, pp. 1-18.
24. G. Thewlis: *Joining Mater.*, 1989, pp. 25-32.
25. S.J. Jones and H.K.D.H. Bhadeshia: University of Cambridge, Cambridge, United Kingdom, unpublished research, 1996.